Quantitative Comparison of Fast Wave Antenna Loading in DIII-D with Theoretical and Computational Models Incorporating Measured Profiles

R.I. Pinsker[1], D. Milanesio[2], R. Maggiora[2], N. Commaux[3], E.J. Doyle[4], G.R. Hanson[3], A. Nagy[5], M. Porkolab[6], P.M. Ryan[3], and L. Zeng[4]

[1]General Atomics, PO Box 85608, San Diego, California 92186-5608, USA
[2]Politecnico di Torino, Dipartimento di Elettronica, Torino, Italy
[3]Oak Ridge National Laboratory, PO Box 2008, Oak Ridge, Tennessee 37831, USA
[4]University of California Los Angeles, Los Angeles, California 90095-7099, USA
[5]Princeton Plasma Physics Laboratory, P.O. Box 451, Princeton, New Jersey 08543, USA
[6]Massachusetts Institute of Technology, Cambridge, Massachusetts 02139, USA

Plasma heating using compressional Alfvén waves ["fast waves" (FWs)] in the ion cyclotron range of frequencies is well-established in magnetic confinement devices and is part of the ITER day-one heating system. In most cases, the limit on the achievable power density that can be coupled by inductive wave launchers is determined by the maximum sustainable rf voltage in the antenna system. The parameter that determines the peak antenna voltage for a given applied rf power is the antenna load resistance, which may be defined as $R_{\mathrm{L}} \equiv 2Z_0^2 P_{\mathrm{c}} / V_{\mathrm{max}}^2$, in which the power coupled to the plasma is P_{c} and the maximum rf voltage in the feedline of characteristic impedance Z_0 is V_{max}. The power limit at fixed V_{max} scales directly with R_{L}, and since V_{max} is generally limited with fixed antenna and feedline geometry, it is essential to have a detailed understanding of the relationship between the edge parameters and the load resistance R_{L}.

To attain such a quantitative understanding of the antenna loading, a detailed model of one of the three existing DIII-D four-element phased array FW antennas was constructed based on the CAD drawings of the structure. Next, the model was exported to the *TO*rino *P*olitecnico *IC A*ntenna (TOPICA) code [1], which incorporates a fully self-consistent electromagnetic model of the antenna structure and a kinetic one-dimensional model of the plasma. Given radial profiles of all of the plasma quantities as input, TOPICA predicts all of the observable electrical properties of the antenna, including the resistive and the reactive components of each element's loading and the mutual coupling between the elements in the phased array.

Before analysing the properties of the plasma-loaded antenna, we compare the TOPICA predictions of the electrical properties of the antenna in vacuum to detailed measurements (performed in the absence of plasma) in order to benchmark the CAD model of the antenna structure. The two-port scattering matrix elements of pairs of the four elements in the phased array were measured from 0.3 MHz to 100 MHz with a vector network analyser and compared with TOPICA calculations carried out at a set of discrete frequencies in the 50–70 MHz band. While excellent agreement was obtained between the predicted and measured phase of the reflection coefficient, at first the magnitude of the voltage transmission

coefficient between toroidally adjacent elements in the array was underestimated by roughly an order of magnitude, signifying that the reactive coupling between elements was larger than initially predicted. This led to the discovery of a discrepancy between the CAD drawings of the antenna that had been used to generate the TOPICA model and the as-built antenna — radial slots in the septa that had been introduced to increase the mutual inductance between elements #1–2 and #3–4 had been omitted from the CAD model. Upon correction of the model to incorporate the slotting of the septa, excellent agreement between all the measured scattering matrix elements and the TOPICA predictions was obtained for the unloaded antenna, thus demonstrating the sensitivity of the observable electrical parameters to details of the antenna geometry, as had also been documented in [2].

Turning to the properties of the plasma-loaded antenna array, the required input is a set of measured plasma radial profiles. Since the FW is essentially a cold plasma mode in the antenna near-field region, the electron and ion temperature profiles have almost no effect on the antenna's predicted electrical properties; the electrical properties are primarily determined by the electron density profile, particularly in the near-field region adjacent to the face of the antenna. Such profiles were obtained in discharges in which the antenna loading was measured with two different profile reflectometer systems. One reflectometer [3] uses an antenna at the same poloidal location as the FW array in a port ~1.5 m away toroidally, while the other reflectometer [4] is immediately adjacent to the FW array. Full sets of profiles and simultaneous antenna loading measurements were obtained in a number of plasma regimes, including L-mode with a range of separatrix/antenna gaps, ELM-free H-mode at a range of gaps and on either side of an L-to-H transition at fixed gap, and QH-mode (an ELM-free quiescent regime) at a single (large) value of gap. Because the FWs are evanescent in the far scrape-off layer (SOL) and propagate only at densities higher than the right-hand cutoff, R_{L} decays exponentially with radial distance from the antenna to the right-hand cutoff layer [5]. R_{L} also depends on the gradient of the density profile just within the propagating region
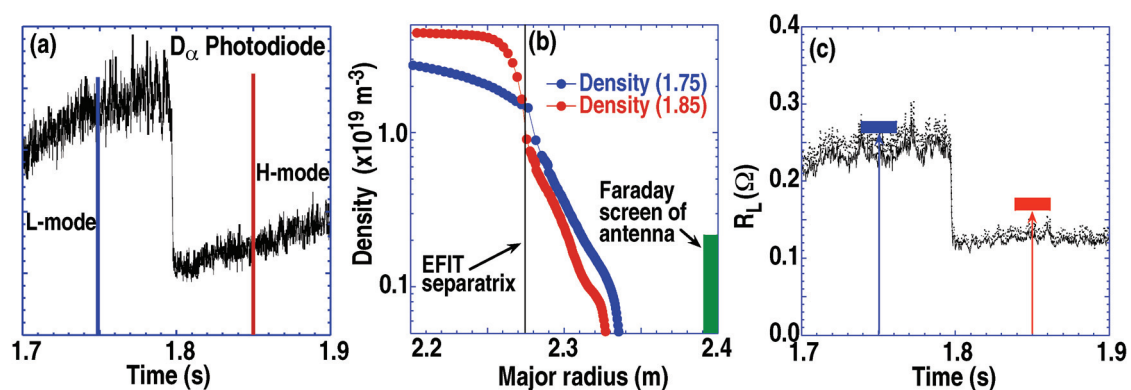

Fig. 1. FW antenna loading just before and just after an L-to-H transition. (a) D_{α} photodiode trace, showing the transition at 1.8 s and the L- and H-mode times at which the density profiles are measured. (b) Semi-log plot of edge density profiles measured with reflectometry. (c) Measured FW antenna loading resistance R_{L} (solid & dashed lines - two independent measurement techniques) and TOPICA predictions at the two timeslices based on the measured density profiles.

("impedance mismatch" or "dielectric mirror" effect), which accounts for the drop in R_L observed at an L-to-H transition [5,6] with a fixed evanescent distance.

To illustrate the analysis procedure, we take the case of antenna loading measured just before and just after an L-to-H transition (Fig. 1). An increase of the neutral beam heating power from 3.2 MW to 4.3 MW at 1.8 s triggers an L-to-H transition, as shown by the sudden decrease in the D_α photodiode signal [Fig. 1(a)]. The density profiles [Fig. 1(b)] at the L-mode timeslice (1.75 s) and H-mode timeslice (1.85 s) measured with the reflectometer adjacent to the FW antenna combined with Thomson scattering show a significant steepening of the density gradient just within the propagating zone. For the parameters of this case (central toroidal field = 2.0 T (field near the antenna = 1.4 T), applied frequency = 60 MHz, principal parallel index of refraction $n_\parallel \approx 5$, deuterium plasma), the FW propagates[*] for electron density greater than $\approx 1 \times 10^{18}$ m^{-3}. The distance from the Faraday screen to the propagating zone increases by about 1 cm as well. Both the steeper gradient in the propagating zone and the increased evanescence contribute to the decrease in R_L that is evident in the measured traces of R_L [Fig. 1(c)].

Inputting the density and other plasma profiles and parameters into TOPICA yields the predictions of antenna loading R_L indicated by the blue (L-mode) and red (H-mode) bars in Fig. 1(c). Taking into account the sensitivity of the predicted loading to the position of the density profile relative to the antenna (difficult to determine precisely from reflectometer data [3,4]), and the fact that the loading at this fairly large gap is only 2–3 times the vacuum (resistive) loading, which has been subtracted from the measured total loading to yield R_L, the level of absolute agreement between TOPICA and experiment is very good.

Data on loading and simultaneous measurements of edge and SOL density profiles were also obtained in an L-mode discharge during which the Faraday screen/separatrix gap was swept during the FW pulse. The measured density profiles and the measured values of R_L are shown in Fig. 2, along with the values
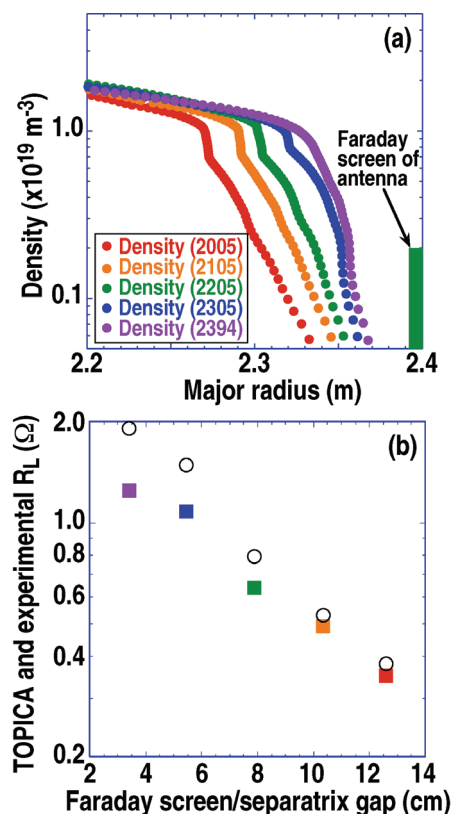

Fig. 2. (a) Density profiles and (b) R_L from dynamic antenna-plasma gap scan in L-mode, with experimental values in open circles, TOPICA in filled squares.

---

[*] For frequencies much lower than the electron cyclotron resonance frequency, the right-hand cutoff density for a pure deuterium plasma is given by $n_e|_{RHC}$ (m^{-3}) = $3.46 \times 10^{14} B_T (f_{MHz} + 7.62 B_T)(n_\parallel^2 - 1)$, where B_T is the local magnetic field in T, f_{MHz} is the FW frequency in MHz, and $n_\parallel \equiv k_\parallel c / \omega$ is the launched index of refraction along the static magnetic field.

predicted by TOPICA using the measured density profiles. Since it is not possible to directly measure the loading resistance R_L, only to calculate R_L from the observable quantities in the transmission line system that feeds the antenna, it is necessary to model the transmission line system in detail, including the diagnostics (directional couplers and voltage probes) and incorporating knowledge of the exact electrical lengths and impedances of all of the sections of the system. Imprecise knowledge of these parameters yields systematic error in the values of R_L that are derived from the measurements. This kind of systematic error may account for the discrepancy between the TOPICA prediction and the experimental value that appears at the smallest values of the Faraday screen/separatrix gap in this scan.

The results of similar analyses of all of the cases so far are summarized in Fig. 3, ranging from L-mode with a small plasma/antenna gap (highest loading) to QH-mode with a very large gap (lowest loading). The 45-degree line represents perfect agreement between the experimentally determined loading and that predicted by TOPICA. It should be noted that the details of the measured density profiles derived from reflectometry (particularly in the vicinity of the right-hand cutoff density, in the far SOL), to which the predicted antenna loading is very sensitive, depend on choices made in the reflectometer data analysis. These reflectometer analysis choices have been optimized for the plasma core and need to be reoptimized for the SOL region, a process which is ongoing. Considering
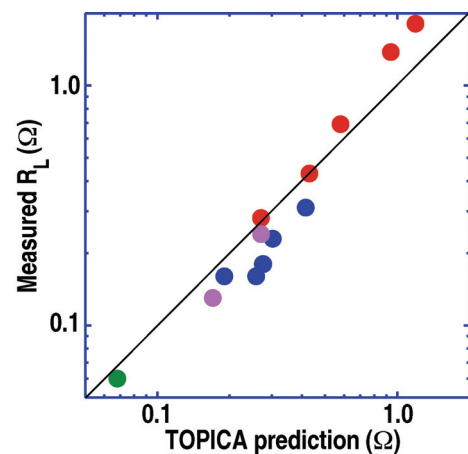

Fig. 3. Comparison of TOPICA computations and experimental results, with QH-mode (green), the two L- and H-mode points from Fig. 1 (magenta), the L-mode dynamic gap scan (red), and a dynamic gap scan in standard ELM-free H-mode (blue).

that there are no adjustable parameters in TOPICA, the level of absolute agreement between the experiment and predicted loading is very good, indicating that a quantitative understanding of the FW coupling process is in hand, given accurate knowledge of the edge density profiles. Consequently, TOPICA may be used to optimize ICRF antenna designs for present-day machines, ITER, and next-step devices.

[1] V. Lancellotti, D. Milanesio, R. Maggiora, *et al.*, Nucl. Fusion **46**, S476 (2006).
[2] D. Milanesio and R. Maggiora, Nucl. Fusion **50**, 025007 (2010).
[3] L. Zeng, G. Wang, E.J. Doyle, *et al.*, Nucl. Fusion **46**, S677 (2006).
[4] G.R. Hanson, *et al.*, Radio Frequency Power in Plasmas (Proc. 11th Top. Conf., Palm Springs, CA, 1995*)* (AIP, NY, 1996) 463.
[5] M.J. Mayberry, S.C. Chiu, R.I. Pinsker*, et al.*, Nucl. Fusion **30**, 579 (1990).
[6] A. Parisot, S.J. Wukitch, P. Bonoli, *et al.*, Plasma Phys. Control. Fusion **46**, 1781 (2004).